Respiratory Research

RESEARCH

Open Access

Lactate activates ER stress to promote alveolar epithelial cells apoptosis in pulmonary fibrosis

Zhiheng Sun[1,2*], Wanyu He[1,2], Huiwen Meng[1,2], Zhihua Ji[1,2], Junxing Qu[3,4*] and Guoying Yu[1,2*]

Abstract

Pulmonary fibrosis (PF) is a chronic, progressive lung disease characterized by fibroblast proliferation, extensive extracellular matrix and collagen deposition, accompanied by inflammatory damage, ultimately leading to death due to respiratory failure. Endoplasmic reticulum (ER) stress in pulmonary fibrotic tissue is indeed recognized as a significant factor exacerbating PF development. Emerging evidences indicated a potential association between ER stress induced by lactate and cellular apoptosis in PF. However, the mechanisms in this process need further elucidation. In this paper, pulmonary fibrosis model was induced by bleomycin (BLM) intratracheally in mice. In the cellular model, type II epithelial cells were treated by lactate and TGF-β to detect ER stress and apoptosis markers. Lactate could promote ER stress response and apoptosis. Mechanically, lactate activated Caspase-12 via ATF4-Chop axis to induce cell apoptosis and promote fibrosis. ER stress inhibitor could effectively suppress alveolar epithelial cells apoptosis and pulmonary fibrosis. We concluded that pro-fibrotic properties of lactate are associated with alveolar epithelial cells apoptosis by causing ER stress and thus provide new potential therapeutic targets for pulmonary fibrosis.

Keywords Pulmonary fibrosis, Lactate, Endoplasmic reticulum stress, Caspase-12, Alveolar epithelial cells, Apoptosis

Introduction

Pulmonary fibrosis (PF) is a chronic, irreversible interstitial lung disease, the etiology of which has not been fully elucidated. Its hallmark is the abnormal deposition of fibrous tissue in the lung parenchyma, accompanied by significant morbidity and poor prognosis [1]. Also, PF is accompanied by generation of a significant number of fragile type II alveolar epithelial cells. These cells demonstrated characteristics of proliferation and differentiation into AT1 cells, accompanied by myofibroblast activation and matrix deposition. The repeated occurrence of repair reactions leads to the formation of scars and loss of lung structural stability, ultimately resulting in PF [2, 3].

Lactate, as the main product of glycolysis and an important signaling molecule, played a key role in tumor progression and cell fate determination [4, 5]. Lactate, as a metabolic product, its accumulation in lung tissue may affect cell survival and function. The accumulation of lactate may affect the microenvironment of lung tissue, thereby promoting the process of fibrosis [6, 7]. The high oxidative state of AECII manifested in a preference for lactate as the metabolic substrate for mitochondrial ATP

*Correspondence:
Zhiheng Sun
sunzhiheng@htu.edu.cn
Junxing Qu
qujx@xxmu.edu.cn
Guoying Yu
guoyuying@htu.edu.cn
[1] College of Life Science, Institute of Biomedical Science, Henan Normal University, Xinxiang, Henan, China
[2] State Key Laboratory of Cell Differentiation and Regulation, Xinxiang, Henan, China
[3] Institutes of Health Central Plains, Xinxiang Medical University, Xinxiang, Henan, China
[4] Xinxiang Key Laboratory for Tumor Drug Screening and Targeted Therapy, Xinxiang, Henan, China

production. Previous studies have shown that the lactate content in the lungs was elevated in PF [8]. The metabolic dysregulation of AEC2 cells was one of the main driving factors for the progression of PF. Glycolytic enzymes, especially lactate dehydrogenase (LDH), could serve as therapeutic targets to help combat the pro-fibrotic environment, thereby inhibiting the differentiation of fibroblasts into myofibroblasts [9].

Apoptosis plays an important role in many physiological processes [10, 11]. The apoptosis of epithelial cells is a key process in various organ fibrotic diseases, including the lungs [12, 13]. During the process of fibrosis, the epithelial cells apoptosis may cause damage to the epithelial layer and an imbalance in repair mechanisms, thereby promoting the PF. Subsequent studies have shown that limiting the loss of AT2 cell function through drug or gene inhibition of the apoptosis pathway also alleviated fibrosis in mice [14]. These observations strengthened a theory that disrupting alveolar epithelial homeostasis promotes the development of pulmonary fibrosis [15, 16]. However, these studies did not explain how dysfunctional AT2 cells, apart from apoptosis, contribute to the development of IPF [17, 18].

ER is the cell organelle responsible for synthesizing, folding, and modifying secretory proteins and transmembrane proteins. Any stimulations may disrupt its protein folding ability, leading to ER stress, such as hypoxia, lactate, accumulation of reactive oxygen species, and disruption of calcium ion homeostasis [19–21]. ATF4 (Activating Transcription Factor 4) is regulated by various stimuli and stress, including ER stress, oxidative stress, and nutrient limitation in cells. Once the cell is under stress, it can regulate the transcription of multiple genes to cope with the challenges. CHOP, also known as C/EBP (CCAAT-enhancer-binding protein)—homologous protein. It is a key target for activating the ATF4 pathway [22]. Caspase-12 is one of the proteins on the outer membrane of the ER, which cannot be activated in the membrane receptor and pathway. It is a specific apoptotic pathway for ER stress and it is the final execution molecule mediating cell apoptosis induced by ER stress [23]. Caspase-12 mediates cell apoptosis through activation of caspase-9 and caspase-3, and can promote ERS-related apoptosis. Research has found an association between CHOP and caspase-12, with overexpression of CHOP promoting the cascade reaction of caspases, releasing caspase-12, ultimately leading to apoptosis in cells. ER stress may promote PF through multiple types of lung cells, including alveolar epithelial cells, fibroblasts, and macrophages [13].

In this study, we treated A549 cells with lactate and detected the expression of ER stress markers and apoptotic proteins to explore the relationship between lactate, ER stress and apoptosis. The data revealed that lactate induced apoptosis was mediated by ER stress. ER stress induced the activation of ATF4-Chop axis, which was responsible for activating Caspase-12 and enhancing Bax expression, while downregulating Bcl-2. Additionally, ER stress inhibitor (4-PBA) could alleviate alveolar epithelial cells apoptosis and suppress PF. Here, we clarified lactate induced alveolar epithelial cells apoptosis to promote PF via ATF4-Chop-Caspase12 axis by causing ER stress. These data may provide us with new insights of PF development and possible targets for PF treatment.

Materials and methods

Reagents and antibodies

Lactate was obtained from Sigma (St. Louis, MO, USA), Antibody against Caspase-12 (#35965) was purchased from Cell Signaling Technology (Boston, MO, USA). Antibody against CHOP (#66741-1-Ig), Bax (#50599-2-Ig), Bcl-2 (#68103-1-Ig) and ATF4 (#60035-1-Ig) were purchased from Proteintech (Wuhan, China). Antibody against PERK (#AF5304), Phospho-PERK (Thr982) (#DF7576), IRE1 (#DF7709), Phospho-IRE1 (Ser724) (#AF7150) and β-Actin (#AF7018) were purchased from Affinity (Changzhou, China).

Cell culture

The A549 cell line of lung epithelial cells and mouse alveolar epithelial cells MLE were obtained from the Type Culture Collection Center at Shanghai Institute of Life Sciences, Chinese Academy of Sciences. The cells were cultured in complete medium consisting of DMEM/F12 basal medium, 1% penicillin–streptomycin solution (100 U/ml penicillin and 100 μg/ml streptomycin), and 10% FBS (fetal bovine serum). The cells were maintained under controlled conditions with a temperature of 37 ℃, 95% air, and 5% CO_2. Upon reaching ~ 70% cell density, they were utilized for subsequent experiments and seeded onto various types of cell plates. These cells were used 10 ng/ml TGF-β from Shanghai Novo Protein to establish a fibrosis model in vitro and were pre-treated with drugs including 10 mM lactate, 500 nM 4-PBA, and 50 μM Cinchonine purchased from Medchem Expression in New Jersey, USA.

Mice

All animal experiments in this manuscript were approved by the Biology Academic Committee of Henan Normal University. The female C57BL/6 mice were utilized as experimental model. All experimental animals were housed in SPF-level animal laboratories and managed according to international protocols for the use and protection of animals. During the experiments, the mice were randomly divided into different experimental

groups and housed under the same environmental conditions. The mice had free access to food and water, with an environmental temperature maintained between 22 °C and 24 °C, a relative humidity of 40–60%, and a 12-h light–dark cycle. Throughout the experiment, strict adherence to ethical standards for animal experimentation was followed in order to minimize pain and suffering for the animals.

Quantitative RT-PCR analysis

Total RNA was extracted from tissues and cells using Trizol reagent. Subsequently, 1μg of RNA was reverse transcribed using HiScript II Reverse Transcriptase (Vazyme, Nanjing, China). The resulting complementary DNA was utilized for real-time PCR amplification on a Fast Real-Time PCR System using Hieff qPCR SYBR Green Master Mix (Yeasen Biotechnology, Shanghai, China). The oligonucleotide primers used for qPCR amplification were listed in Table 1. The relative expression levels of the target genes were determined using the $2^{-\Delta\Delta Ct}$ method. All experiments were performed with three replicates.

Western blot

Proteins were extracted from tissues and cells using RIPA buffer, and their concentrations were quantified using the Pierce BCA Protein Assay Kit (Thermo Scientific). The protein lysates were separated on 10–15% SDS–polyacrylamide gels, with a loading of 20–50 μg each time. After electrophoresis, the proteins were transferred onto polyvinylidene fluoride membranes (Millipore, Billerica, MA, USA), followed by blocking with non-fat milk powder at room temperature for 1 h to prevent non-specific binding. Subsequently, the membranes were incubated overnight at 4 °C with specific primary antibodies as described previously based on the target band size. β-actin was used as an internal control. On the next day, the bands were washed three times with TBST buffer and then treated with HRP-conjugated secondary antibodies at room temperature for 2 h. After three additional washes with TBST buffer, immunoreactivity was detected using Thermo Scientific's enhanced chemiluminescence (ECL) Western blotting detection reagents and visualized using the Odyssey® XF imaging system.

Immunohistochemistry

In the PF model, immunohistochemical staining was performed on mouse lung tissue slices. These slices were fixed with formalin, embedded in paraffin, and processed according to standard procedures. The following antibodies were used: anti-CHOP (1:100, Proteintech, Wuhan, China), anti-ATF4 (1:100, Proteintech, Wuhan, China), anti-Phospho-PERK (Thr982) (1:100 Affinity, Jiangsu Province of China), anti-Phospho-IRE1 (Ser724) (1:100 Affinity, Jiangsu Province of China), and anti-Caspase-12 (1:100 CST Boston USA).

Immunofluorescence staining

The cultured cells were seeded onto glass slides and placed in a 24-well plate for incubation in a CO_2 incubator. After three washes with PBS, the samples were fixed with 4% paraformaldehyde at room temperature for 15 min. Following fixation, the cells were washed with PBS and then incubated in a glycine solution prepared with PBS to react with aldehydes. Subsequently, the cells were washed three times with PBS and incubated in a 0.3% Triton X-100 solution at 4 °C for 10 min to increase permeability. After permeabilization, non-specific binding was blocked by incubating the samples in a 5% BSA solution at room temperature for one hour. Primary antibodies against Caspase-12 and CHOP were diluted at a

Table 1 Primer sequences

Gene	Sense (5′–3′)	Anti-sense (5′–3′)
M-Col1a1	GCTCCTCTTAGGGGCCACT	CCACGTCTCACCATTGGGG
H-CASP12	AGAGCCAGATGTTCTTCACGATG	CGGCTTTTCCACTGTCAGTGGT
M-Casp12	CAGATGAGGAACGTGTGTTGAGC	GGAACCAGTCTTGCCTACCTTC
H-BAX	TCAGGATGCGTCCACCAAGAAG	TGTGTCCACGGCGGCAATCATC
H-BCL2	ATCGCCCTGTGGATGACTGAGT	GCCAGGAGAAATCAAACAGAGGC
H-ATF4	TTCTCCAGCGACAAGGCTAAGG	CTCCAACATCCAATCTGTCCCG
M-Atf4	AACCTCATGGGTTCTCCAGCGA	CTCCAACATCCAATCTGTCCCG
H-ATF6	TCCTCGGTCAGTGGACTCTTA	CTTGGGCTGAATTGAAGGTTTTG
M-Atf6	GTCCAAAGCGAAGAGCTGTCTG	AGAGATGCCTCCTCTGATTGGC
H-DDIT3	GGTATGAGGACCTGCAAGAGGT	CTTGTGACCTCTGCTGGTTCTG
M-Ddit3	GGAGGTCCTGTCCTCAGATGAA	GCTCCTCTGTCAGCCAAGCTAG
H-ACTB	GGCTGTATTCCCCTCCATCG	CCAGTTGGTAACAATGCCATGT
M-Actb	CATTGCTGACAGGATGCAGAAGG	TGCTGGAAGGTGGACAGTGAGG

Table 2 Primer sequences

Gene	Sense (5′–3′)	Anti-sense (5′–3′)
H-CHOP	CGCGGATCCATGGAGCTTGTTCCAGCCA	CCGCTCGAGCGTCATGCTTGGTGCAGATTCA
H-ATF4	TGGAATTCTGCAGATATGACCGAAATGAGCTT	GCCACTGTGCTGGATCTAGGGGACCCTTTTCTTC
H-ATF5	CGGGGTACCATGTCACTCCTGGCGACCCT	CCGCTCGAGCTAGCAGCTACGGGTCCTCT
H-ATF6	TGGAATTCTGCAGATATGGGGGAGCCGGCTGGGGTTG	GCCACTGTGCTGGATCTATTGTAATGACTCAGGGATG

ratio of 1:200 in BSA and reacted overnight at 4 °C for no less than 18 h. Then, the samples were further incubated under dark conditions for an additional hour and a half after being bound by secondary antibodies conjugated with Alexa Fluor 488 and Alexa Fluor594 at dilutions of 1:400. After washing with PBS, cell nuclei were stained using DAPI as a nuclear dye. Finally, the slides were observed using Nikon Eclipse Ti-U fluorescence microscope equipped with DS-Ri1 digital camera.

Cell viability assay

In a 96-well plate, inoculate 100 µl of cell suspension (~ 5000 cells/well). Place the plate in a humidified incubator for pre-culture (e.g., at 37 ℃, 5% CO_2 conditions). Then add 10 µl of the test substance at different concentrations to each well and incubate for an appropriate duration in the incubator (e.g., 6, 12, 24 or 48 h). Finally, add 10 µl of CCK-8 solution to each well. Take care to avoid bubbles entering the wells as they can interfere with OD value detection. Return the culture plate to the incubator for further incubation for 1–4 h. Before reading the plate, gently mix the samples to ensure uniformity. Then measure absorbance at wavelength of 450 nm using an enzyme-linked immunosorbent assay reader and perform data analysis.

Flow cytometry analysis

Cells were cultured in six-well plates and subjected to apoptotic stimulation. Subsequently, cells were harvested by digestion. After washing with PBS, cells were resuspended in 1 × Binding Buffer to adjust the cell concentration of each sample to $1–5 \times 10^6$ cells/ml. Then, 100 µl of cell suspension was taken and mixed gently with 5 µl of Annexin V FITC and PI, and the reaction was carried out at room temperature in the dark for 5 min. After the reaction, 400 µl of 1 × Binding Buffer was added to each sample tube, making the total volume 500 µl. Flow cytometry analysis was performed within one hour after staining.

Annexin V-FITC analysis

Cells were cultured in 24-, 48-, or 96-well plates and subjected to apoptotic stimuli. After removing the cell culture medium, cells were washed once with PBS. Subsequently, 195 µl of Annexin V-FITC binding buffer and 5 µl of Annexin V-FITC were added, and gently mixed. The mixture was then incubated at room temperature in the dark for 10–20 min, followed by placement on ice. Light avoidance was achieved using aluminum foil. Finally, samples were observed under a fluorescence microscope.

H&E staining

Fresh samples were fixed and routinely embedded in paraffin, then sliced into 3–8 µm sections. Dewaxing was performed twice in xylene for 5–10 min each time. The sections were rehydrated with a series of ethanol gradients (100%, 95%, 85%, 75%) for 3 min per gradient. They were soaked in distilled water for 2 min. Staining with hematoxylin was carried out for 2–20 min, followed by rinsing off the excess stain with distilled water. Differentiation solution was applied for 10–60 s, followed by two washes with tap water or immersion for a total of 3–5 min each time. The sections were then stained with eosin for 30 s to 2 min, excess staining liquid was poured off quickly, and the slides were dehydrated rapidly, cleared, and mounted.

(See figure on next page.)

Fig. 1 BLM-induced PF is accompanied by lactate accumulation and epithelial cells apoptosis. **A** PF model was established in mice with 2 U/kg bleomycin or 0.9% normal saline (50 µl) in vivo (n = 3). **B** Masson's trichrome staining and H&E staining of representative lung sections (n = 3) from each group of treated mice, scale bar: 20 µm. **C** Lactate content in broncho alveolar lavage fluid (BALF) were measured. ****$p < 0.0001$, compared with saline group. **D** The mRNA levels of *Col1a1* of mice lung were detected by qPCR (n = 3). **$p < 0.01$, compared with saline group. **E** Immunohistochemical mice lung Caspase-12 staining in saline and BLM group, scale bar: 20 µm. **F** The mRNA levels of *Casp12* of mice lung were detected by qPCR (n = 3). **$p < 0.01$, compared with Saline group. **G** The protein expression of Apoptosis and ER stress markers were measured by western blot. β-Actin was used as a loading control. **$p < 0.01$, ***$p < 0.001$, compared with saline group. **H** Apoptosis was detected in alveolar epithelial cells using reporter mice. Nucleus (blue), FITC (green), SP-C (red), scale bar: 200 µm

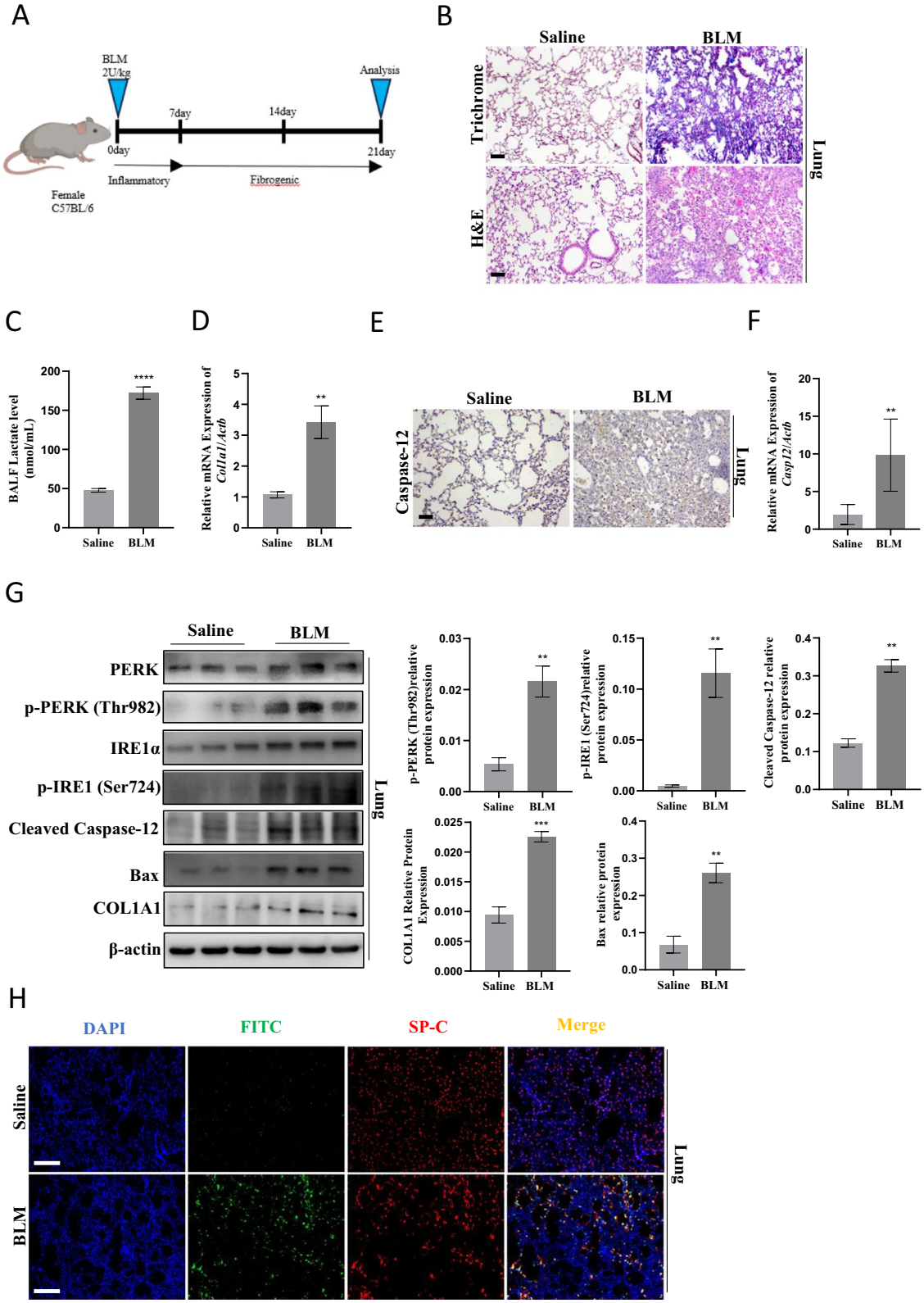

Fig. 1 (See legend on previous page.)

Masson's trichrome staining

Slice the wax off until water. Treated the slices with reagents separately, referring to the instruction manual for specific steps. (Solarbio, Beijing, China).

Hydroxyproline assay

The Sigma-Aldrich hydroxyproline assay kit (MAK008) was used to assess the total lung collagen levels. In brief, mouse lung tissue was homogenized in H_2O to a concentration of 100 mg/ml. Approximately 100 µl of the homogenate was mixed with 100 µl of 12 M HCl and subjected to a hydrolysis reaction at 120 °C for 3 h. Subsequently, the hydroxyproline content in ~ 10 µl of the sample was analyzed according to the manufacturer's instructions.

Plasmid transfection

Overexpression plasmids of CHOP and ATF5 were constructed in the Phage flag. Overexpression plasmids of ATF4 and ATF6 were constructed in the pc DNA 3.1. The CHOP promoter was constructed in the PGL-3. Primer sequences for plasmids construction used were listed in Table 2. Transient transfection of control plasmid or overexpression plasmids was performed using Lipofectamine 3000 (Invitrogen) according to the manufacturer's instructions.

Dual luciferase reporter gene assay

Construct the corresponding vector. Please refer to the relevant manual for transfection steps. Thoroughly mix the cell lysis solution and add it according to the manual, fully lysing the cells. Follow the instructions for operation (Yeasen, Shanghai, China).

Statistics

All data were analyzed using Graphpad Prism 8 software (GraphPad Software, located in Los Angeles, CA, USA) and presented graphically. Data were presented as mean ± standard deviation (SD). All data followed the assumption of normal distribution. For comparisons between two groups, statistical analysis was performed using a two-tailed Student's t-test. For comparisons among three or more groups, one-way analysis of variance (ANOVA) was used followed by Tukey's test to assess significant differences. A p-value less than 0.05 was considered statistically significant.

Results

BLM-induced PF is accompanied by lactate accumulation and epithelial cells apoptosis

Previous studies have shown that lactate levels increased during PF. To further confirm the role of lactate in fibrosis development, we established a mouse model of PF induced by BLM (Fig. 1A). We observed more abnormal collagen accumulation and more severe lung injury in the BLM-treated group (Fig. 1B). At the same time, the lactate content in the bronchoalveolar lavage fluid of the BLM-treated group was higher than the control group and the *Col1a1* mRNA level was upregulated (Fig. 1C, D). Caspase-12 is a final executioner molecule of ER (ER) stress-mediated cell apoptosis, which can be activated by ER stress apoptotic signals, including disruption of ER calcium ion balance and accumulation of excess proteins in the ER. Immunohistochemistry and qPCR results showed upregulation of Caspase-12 in lung (Fig. 1E, F). Western blot showed that in the mice treated with BLM, the level of collagen deposition was higher, ER stress upregulated, increased levels of cleaved Caspase-12, and enhanced Bax expression (Fig. 1G). Additionally, apoptosis was detected in alveolar epithelial cells using reporter mice (Fig. 1H).

Lactate induced alveolar epithelial cells apoptosis in vitro

TGF-β (transforming growth factor-beta) is a cytokine that plays a crucial role in the occurrence and development of many diseases, including cancer, immune-related diseases, and fibrosis. We treated A549 cells with TGF-β to simulate in vitro. The results showed that TGF-β treatment could activate the activity of Caspase-12, consistent with in vivo results (Fig. 2A). To investigate the effect of lactate on cell viability, we treated the cells for 24 and 48 h. With the increase in time, lactate significantly inhibited cell viability. Under the combined action of TGF-β and lactate, cell viability was significantly lower than that in the TGF-β group (Fig. 2B). Subsequently, we stimulated A549 cells with 10 mM lactate for 48 h and the results showed that enhanced Caspase-12 and Bax expression

(See figure on next page.)

Fig. 2 Lactate induced alveolar epithelial cells apoptosis in vitro. **A** The protein expression of Cleaved caspase-12 was measured by western blot in A549 cells. **p < 0.01, compared with control group. **B** The effect of Lactate and TGF-β (5 ng/ml) on A549 cells viability for 48h were tested with CCK-8 assay kit (n = 3). **C**, **D** The protein expression of Apoptosis markers was measured by western blot in both A549 and MLE cells. *p < 0.05, **p < 0.01, compared with control group. **E** The apoptosis rate was significantly increased in A549 cells from both control and lactate groups (n = 3/group). ***p < 0.001, compared with control group. **F** The apoptosis status in A549 cells was assessed using Annexin V-FITC apoptosis detection kit by fluorescence microscopy, scale bar: 200 µm

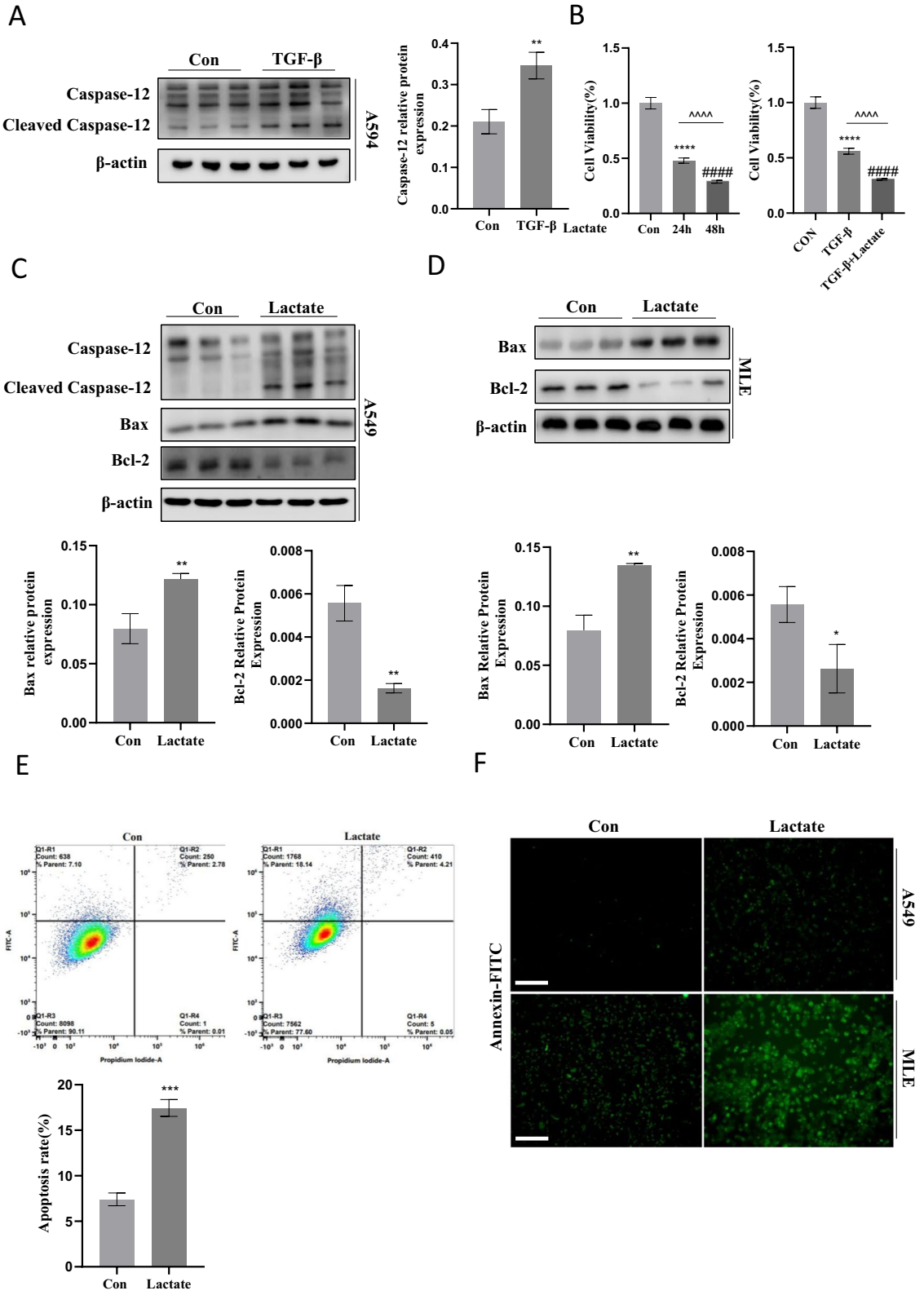

Fig. 2 (See legend on previous page.)

and downregulation of Bcl-2 (Fig. 2C). Similarly, mouse epithelial cells (MLE) showed similar results, with upregulation of Bax and downregulation of Bcl-2 (Fig. 2D). Flow cytometry analysis revealed a higher proportion of apoptotic cells (Fig. 2E). Annexin V-FITC staining showed more green fluorescence in both A549 cells and MLE cells treated with lactate, indicating that lactate could promote apoptosis of epithelial cells (Fig. 2F). Moreover, we found a significant decrease in E-cadherin protein expression and an increase in N-cadherin protein expression in TGF-β treated A549 cells. And, we cultured fibroblasts with epithelial cell conditioned medium (TGF-β treated) and normal epithelial cell medium, western blot results demonstrated a significant upregulation of the Fibronectin, COL1A1 and α-SMA (Supplementary Fig. 1A). The findings suggested that lactate promoted apoptosis of alveolar epithelial cells in vitro.

Lactate induced ER morphological changes and ER stress in alveolar epithelial cells.

PERK (Protein kinase RNA-like ER kinase) and IRE1 (Inositol-requiring enzyme 1) are two key proteins in the ER stress response, and their activity is determined by the phosphorylation status of residues at threonine 982 and Serine 724. They played crucial roles in regulating cellular responses to ER stress. Firstly, we observed upregulation of Phospho-PERK (Thr982) and Phospho-IRE1 (Ser724) in BLM-induced pulmonary fibrosis model (Fig. 3A). The previous research has shown that lactate induced apoptosis of epithelial cells, we stimulated A549 cells with 10 mM lactate and detected the activation status of ER stress markers (PERK, IRE1 and ATF6). The results showed upregulation of Phospho-PERK (Thr982) and Phospho-IRE1 (Ser724) expression (Fig. 3B). Moreover, we detected the expression of ATF6. In the bleomycin-induced mouse fibrosis model, the mRNA levels of *Atf6* were upregulated and lactate treatment also led to an upregulation of *ATF6* mRNA levels (Supplementary Fig. 1B, C). Additionally, we observed the morphology of the ER under stress conditions, and the results showed changes in the morphology of the ER under lactate stimulation (Fig. 3C). Subsequently, in the TGF-β-induced cell model, the results showed that in the TGF-β + lactate group, the expression levels of Phospho-PERK (Thr982) and Phospho-IRE1 (Ser724) were significantly upregulated (Fig. 3D). There are related studies showing that Caspase-12 is located on the cytoplasmic side of the ER membrane [12]. Lactate treatment could promote the entry of Caspase-12 into the nucleus (Fig. 3E). These data suggested that lactate induced ER morphological changes and ER stress in alveolar epithelial cells.

ER stress inhibitor alleviated lactate-induced cell apoptosis in vitro

Due to lactate-induced ER stress and apoptosis in epithelial cells, we aimed to further validate the role of ER stress in fibrosis. We found that at a concentration of 500 nM, 4-PBA could increase cell viability and alleviate the damage caused by lactate (Fig. 4A). Under the action of the ER stress inhibitor (4-PBA), the mRNA levels of *CASP12* and *BAX* were significantly reduced, while *BCL2* mRNA levels were upregulated (Fig. 4B). Western blot results showed that the Lactate + 4-PBA group inhibited the activity of Caspase-12 in A549 cells, downregulated Bax expression and enhanced Bcl-2 expression in A549 cells (Fig. 4C). Cinchonine is an ER activator that can induce cell apoptosis mediated by ER stress. We stimulated A549 cells with 50 μM Cinchonine and lactate, and the results showed that Cinchonine could induce cell apoptosis, leading to upregulation of *CASP12* and *BAX* mRNA levels and downregulation of *BCL2* mRNA levels. Under co-treatment with Cinchonine and lactate, lactate could exacerbate cell apoptosis (Fig. 4D). Flow cytometry data demonstrated that 4-PBA alleviated lactate-induced apoptosis (Fig. 4E). Similarly, 4-PBA mitigated lactate-induced ER morphological changes (Supplementary Figure C). Scratch data indicated that cell migration of A549 cells was inhibited by lactate treatment, and migration of cells in the Lactate + Cinchonine group was similarly inhibited. Conversely, the use of 4-PBA promoted A549 migration (Fig. 4F, G).

Caspase-12 was activated by the ATF4-Chop *axis* and promoted alveolar epithelial cells apoptosis

The expression of ATF4 (activating transcription factor 4) in cells is regulated by various stimuli and stresses, including ER stress, oxidative stress, and nutrient restriction. While CHOP, also known as C/EBP

(See figure on next page.)

Fig. 3 lactate induced ER morphological changes and ER stress in alveolar epithelial cells. **A** Immunohistochemical mice lung p-PERK (Thr982) and p-IRE1 (Ser724) staining in the bleomycin-induced mouse pulmonary fibrosis model, scale bar: 20 μm. **B** Lactate induced ER stress in A549 cells. *$p < 0.05$, **$p < 0.01$, compared with control group. **C** Lactate induced morphological changes of ER in A549 cells. ER-Tracker (green). Nuclei were counterstained with DAPI (blue), scale bar: 20 μm. **D** The markers of ER stress were detected by Western blot in A549 cells. *$p < 0.05$, ***$p < 0.001$, compared with TGF-β group. **E** Lactate promoted nuclear translocation of Caspase-12 in A549 cells. Caspase-12 (red), nucleus (blue), scale bar: 20 μm

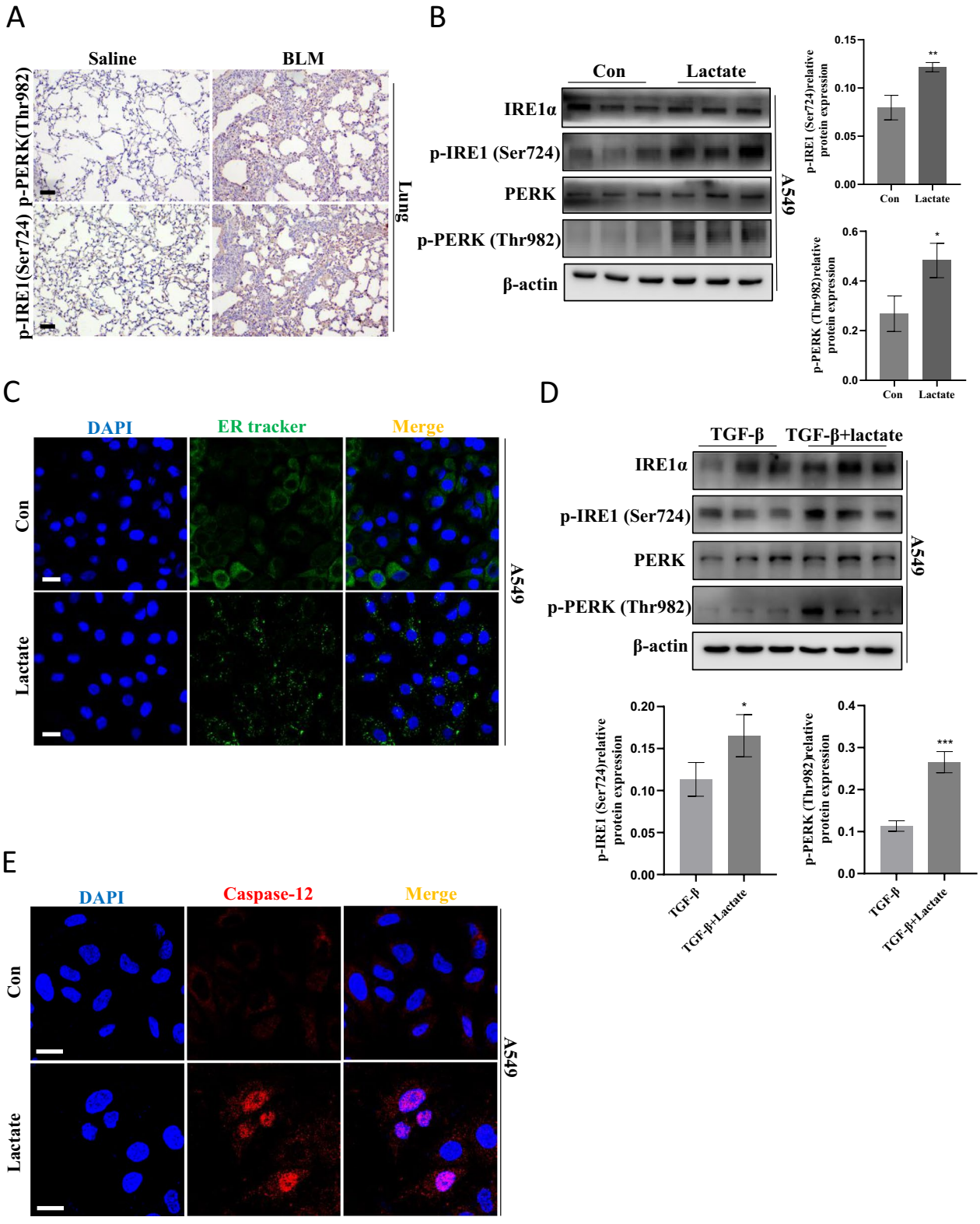

Fig. 3 (See legend on previous page.)

(CCAAT-enhancer-binding protein) or GADD153 (growth arrest and DNA damage-inducible gene 153), is a transcription factor and one of the key targets of the ATF4 pathway. It plays a critical role in switching from anti-apoptotic to pro-apoptotic effects during ER stress. Immunohistochemistry showed upregulation of ATF4 and CHOP in the bleomycin-induced mouse model of PF (Fig. 5A). The mRNA expression levels of *Atf4* and *Ddit3* were increased in lung fibrotic mice by qPCR (Fig. 5B). Subsequently, A549 cells were treated with lactate, which significantly increased the *ATF4* and *DDIT3* mRNA expression levels (Fig. 5C). Similarly, in a TGF-β-induced cellular model, both the protein and mRNA expression levels were significantly upregulated (Fig. 5D, E). To investigate the role of CHOP, overexpression of CHOP in A549 cells enhanced the expression of Caspase-12 and Bax. These results suggested that CHOP could regulate the activation of caspase-12, upregulate Bax, and induce apoptosis (Fig. 5F). Dual luciferase reporter gene assay showed that ATF4 positively regulated the expression of CHOP (Fig. 5G). Furthermore, we assessed the effect of CHOP overexpression on cell migration in A549 cells and found overexpression of CHOP inhibited cell migration (Fig. 5H, I).

ER stress inhibitor could alleviate mice pulmonary fibrosis

To validate the specific effects of the drugs on the mouse fibrosis model, we conducted in vivo experiments on mice (Fig. 6A). On the 7th day post-BLM treatment, mice were intraperitoneally injected with 4-PBA and Cinchonine. Compared to the BLM-treated group, the BLM + Cinchonine treated group exhibited elevated levels of hydroxyproline. 4-PBA significantly reduced the levels of hydroxyproline in fibrotic mouse lungs (Fig. 6B). Similarly, 4-PBA also decreased the levels of *Col1a1* mRNA in the fibrotic mouse bodies (Fig. 6C). HE staining and Masson staining results demonstrated that 4-PBA could diminish the deposition of aberrant collagen in fibrotic mouse lungs and alleviate lung damage. And, the results showed no significant differences compared with saline group and 4-PBA group (Fig. 6D). In addition, 4-PBA also reduced lactate levels in lung tissue of BLM-induced mice (Supplementary Fig. 1E). Subsequently, we validated these findings through Western blotting, which revealed that the use of 4-PBA could inhibit Caspase-12 activity, reduce collagen expression, and upregulate Bcl-2 (Fig. 6E). These results confirmed that inhibiting ER stress could alleviate pulmonary fibrosis in mice.

Discussion

PF is an interstitial lung disease characterized by dysregulated inflammation, progressive scarring of the lungs, and usually progresses to respiratory failure and death within 3–5 years [24]. Otto Warburg first described the process in which tumor tissues produced lactate through aerobic glycolysis and released it into the extracellular space, and later it was found that this metabolic pathway exists in many cell types, including immune cells [25]. Our previous studies have shown that the expression of PDK1 was significantly increased in fibrotic lung tissue, which upregulated the activation of lung fibroblasts and epithelial–mesenchymal transition of alveolar epithelial cells. In addition, the activation of PDK1 also promoted glycolysis, leading to the accumulation of lactate in lung tissue [8]. Previous studies have shown that LDHA is a key enzyme involved in glycolysis, which is elevated in the silica-induced fibrotic model and closely associated with inflammation and silicosis fibrosis. The authors found that oxamate regulated LDHA, which could control macrophage glycolysis and ER stress, thereby reducing lactate production and alleviating pulmonary fibrosis [26]. In recent years, we have gained a deeper understanding of the role of lactate, yet there are still many aspects that require further exploration. Glycolysis and ER stress are considered to be important driving factors for pulmonary fibrosis. However, it is currently unclear whether glycolysis and ER stress are interrelated, and whether these interrelationships regulate the development of pulmonary fibrosis. The relationship between lactate and PF needs to be further elucidated to comprehensively understand lactate.

This study explored the relationship between lactate and apoptosis, and found a connection between them. We found that lactate could act as a signaling molecule in epithelial cells, inducing ER stress and ultimately leading to apoptosis. When cells exposed to multiple stimuli, it

(See figure on next page.)

Fig. 4 ER stress inhibitor alleviated lactate-induced cell apoptosis in vitro. **A** The effect of 4-PBA on cell viability was determined using the CCK-8 assay in A549 cells (n = 5). ***p < 0.001, ****p < 0.0001, compared with control group. ##p < 0.01, ###p < 0.001, compared Lactate group and Lactate + 4-PBA group. **C** The protein expression of Apoptosis markers was measured by western blot with control, Lactate and Lactate + 4-PBA groups in A549 cells. **D** The effect of Cinchonine on apoptosis markers was detected by qPCR (n = 3). **E** The apoptosis rate was significantly reduced in A549 cells compared with the lactate group and lactate + 4-PBA group (n = 3). ****p < 0.0001, compared with control group and lactate group. ####p < 0.0001, compared with lactate group and lactate + 4-PBA group. **F**, **G** The migratory effects of Lactate, 4-PBA, and Cinchonine on A549 cells were detected by using scratch assay

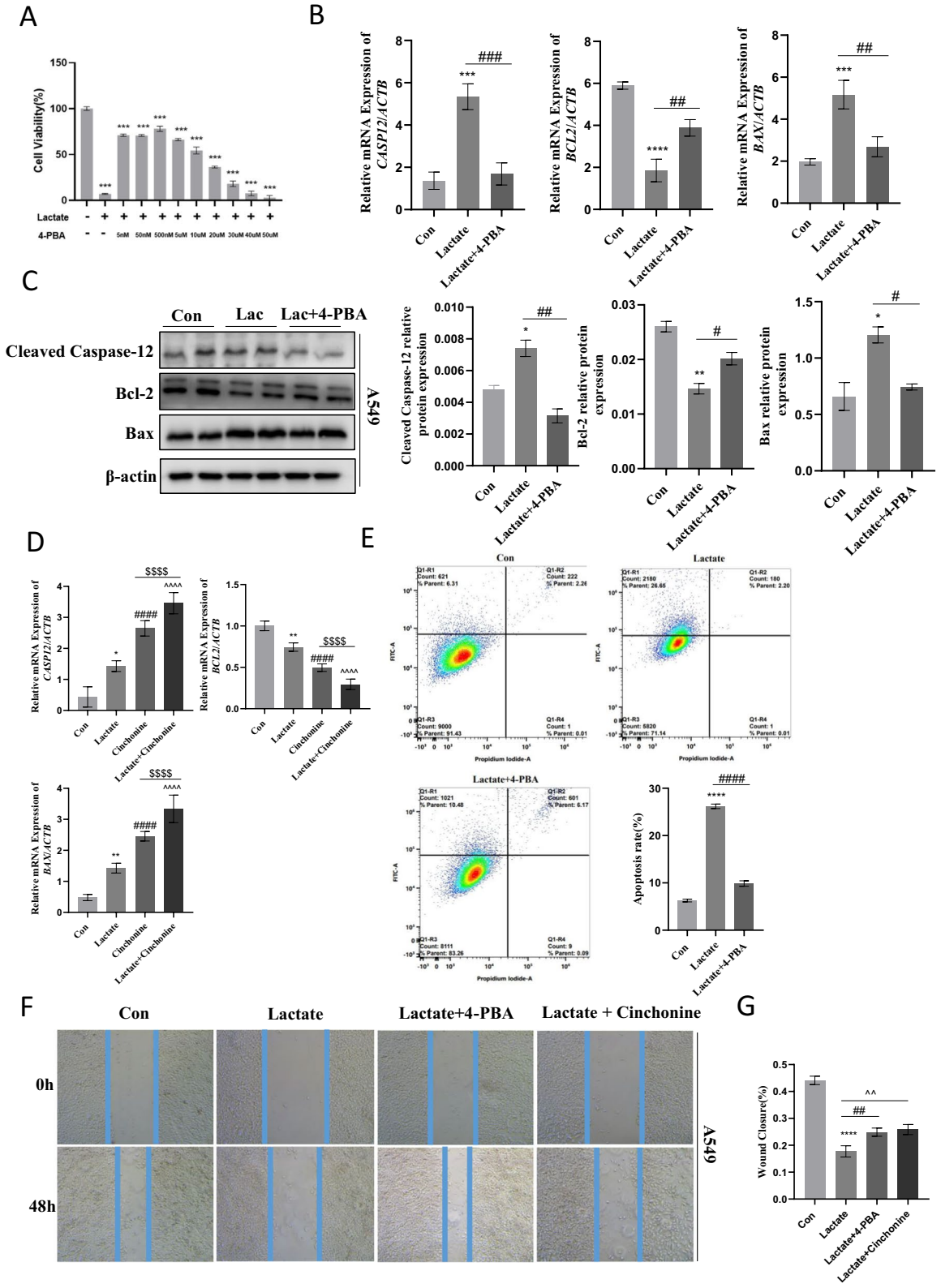

Fig. 4 (See legend on previous page.)

could lead to ER stress. However, there are many causes of ER stress. But this article only focused on lactate. Nevertheless, there are no relevant reports on how lactate regulates ER stress. Our next research goal is to explore the relationship between lactate and ER stress. The release of Ca^{2+} from the ER led to mitochondrial membrane depolarization, resulting in mitochondrial ROS production, which further promoted the accumulation of unfolded proteins in the ER, thereby inducing ER stress [27]. Therefore, our next step is to investigate whether lactate can lead to ROS production, inducing ER stress, and exacerbating PF. Relevant studies reported high expression of ERO1α in cancer, with CHOP being able to regulate its expression. CHOP could upregulate the expression of ERO1α, which catalyzed the re-oxidation of PDI, leading to a highly oxidizing environment in the ER [27]. However, knocking down ERO1α could inhibit cancer cell metastasis [28]. This provided a new perspective for studying the relationship between lactate and ER stress.

Aspartate-specific cysteine protease-12 (caspase-12) is a protein situated on the outer membrane of the ER, involved in a specific apoptotic pathway of ER stress and mediating cell apoptosis through activation of caspase-9 and caspase-3 [29]. This study for the first time found that lactate could activate Caspase-12. CHOP played a crucial role in ER stress by regulating the activation of caspase-12, influencing cell fate by regulating cellular survival and death pathways. ER stress could cause an increase in cytoplasmic calcium levels, which then activated m-calpain. Activated m-calpain cleaved Bcl-XL and hydrolyzed to activate Caspase-12 [23]. Research has shown that caspase-12 was associated with tumor necrosis factor receptor-associated factor-2 (TRAF2) [30]. Therefore, we speculated that m-calpain and TRAF2 may regulate the expression of Caspase-12.

Sodium 4-phenylbutyrate is an inhibitor of histone deacetylase (HDAC) and ER stress, which can reduce Caspase-12. Research reported that 4-PBA significantly inhibited cell apoptosis and autophagy, while ER stress may be an upstream mediator of cell autophagy and apoptosis [31]. In addition, 4-PBA could inhibit the activation of the NF-κB signaling pathway, reduce the release of pro-inflammatory mediators, and significantly suppress LPS-induced inflammatory response, thereby alleviating acute lung injury [32]. Silicon dioxide stimulated ER stress and activated the TLR4-NF-κB pathway, triggering inflammation and leading to PF [33, 34]. In vitro experiments have shown that maintaining ECM homeostasis and alleviating silica -induced mouse fibrosis could be achieved by inhibiting ER stress, inflammatory response and the TLR4-NF-κB pathway, providing valuable insights into the mechanism of fibrosis [33, 35]. Importantly, Lactate has long been considered as a metabolic waste product, Zhao et al. first discovered histone lysine lactylation (Kla) in 2019, which links gene regulation to cell metabolism through dysmetabolic activity and epigenetic modifications, influencing TME and tumor development [36]. The protein lactylation modification played a role in cellular functions related to glycolysis and macrophage polarization and is associated with various diseases including PF [8]. Targeting specific enzymes or pathways for drug intervention to regulate lactylation. As an epigenetic inhibitor, 4-PBA may be worth further investigation as to whether it can improve PF by regulating lactylation. In addition, a deeper understanding of the relationship between lactylation and PF from multiple aspects such as inflammation, fibrosis, and immune response, to improve the condition of patients with PF and provide more effective options for future treatment. However, this study primarily focused on epithelial cells. Nevertheless, fibroblasts and macrophages also play crucial roles in the fibrotic process. The role of ER stress in these cell types remains to be further elucidated. Therefore, considering lactate-induced ER stress and apoptosis as therapeutic targets may be a treatment approach for PF.

Conclusion

Lactate is one of the important factors in PF by affecting alveolar epithelial cells. We found that lactate could induce apoptosis through ER stress in alveolar epithelial cells. The first to identify that lactate activated Caspase-12 via ATF4-Chop axis to induce cell apoptosis. ER inhibitors effectively prevented excessive apoptosis of alveolar epithelial cells and alleviated PF. These findings

(See figure on next page.)

Fig. 5 Caspase-12 was activated by the ATF4-Chop axis and promoted alveolar epithelial cells apoptosis. **A** Immunohistochemical mice lung ATF4 and CHOP staining in saline and BLM group, scale bar: 20 μm. **B** The mRNA expression levels of *Atf4* and *Chop* were detected by qPCR (n = 3). $^{**}p < 0.01$, $^{***}p < 0.001$, compared with saline group. **C** Lactate could increase the mRNA expression levels of *ATF4* and *CHOP* (n = 3). $^{***}p < 0.001$, $^{****}p < 0.0001$, compared with control group. **D** TGF-β could promote the mRNA expression levels of *ATF4* and *CHOP* (n = 3). $^{****}p < 0.0001$, compared with control group. **E** The protein expression of Apoptosis markers was measured by western blot with control and TGF-β groups. $^{****}p < 0.0001$, compared with control group. **F** Over expression CHOP could promote the expression of apoptotic proteins in A549 cells $^{*}p < 0.05$, $^{***}p < 0.001$, compared with control group. **G** ATF4 regulated the expression of CHOP from each group (n = 3), $^{***}p < 0.001$, compared with NC group. **H**, **I** The migratory effects of CHOP overexpression on A549 cells were assessed using scratch assay

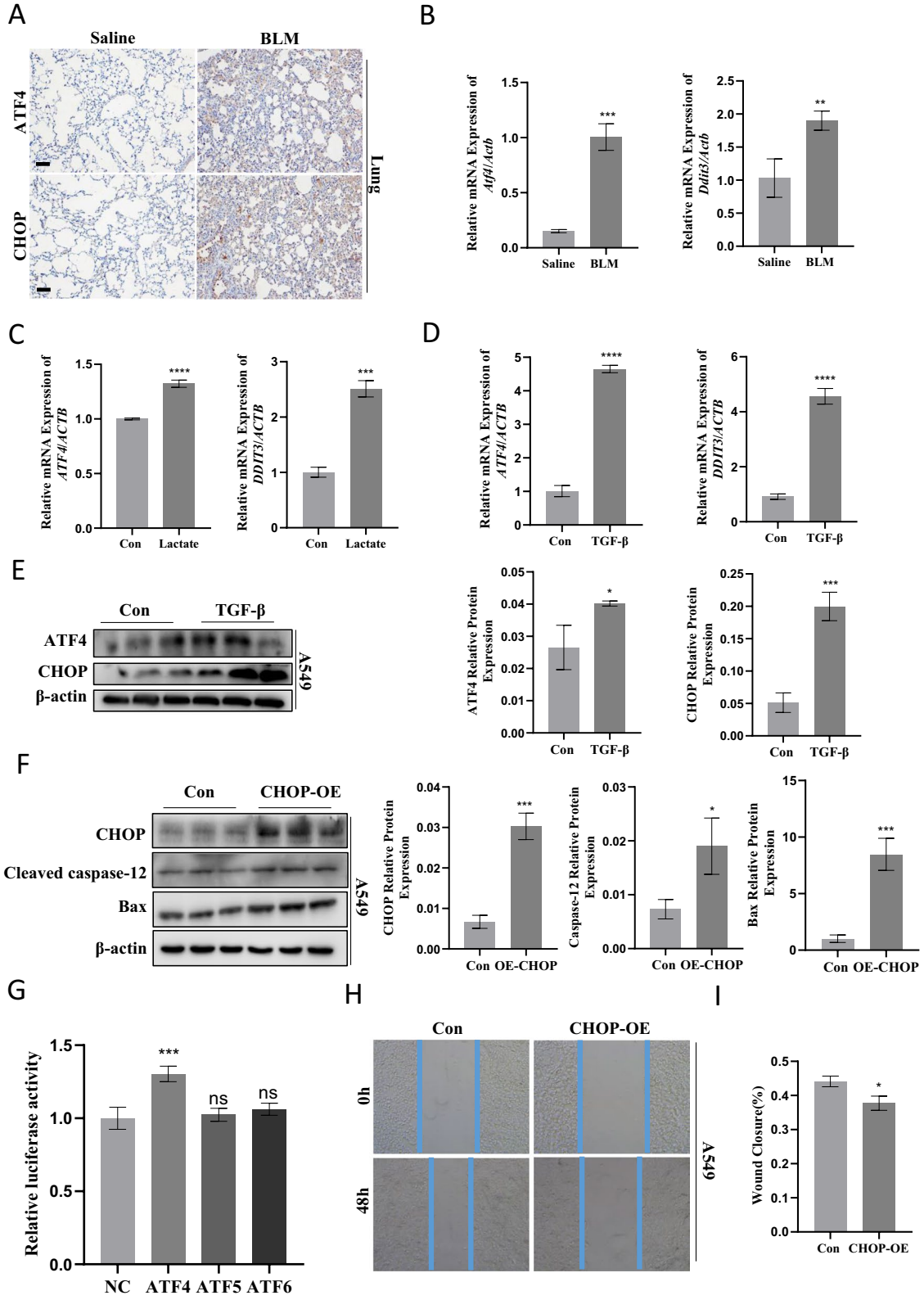

Fig. 5 (See legend on previous page.)

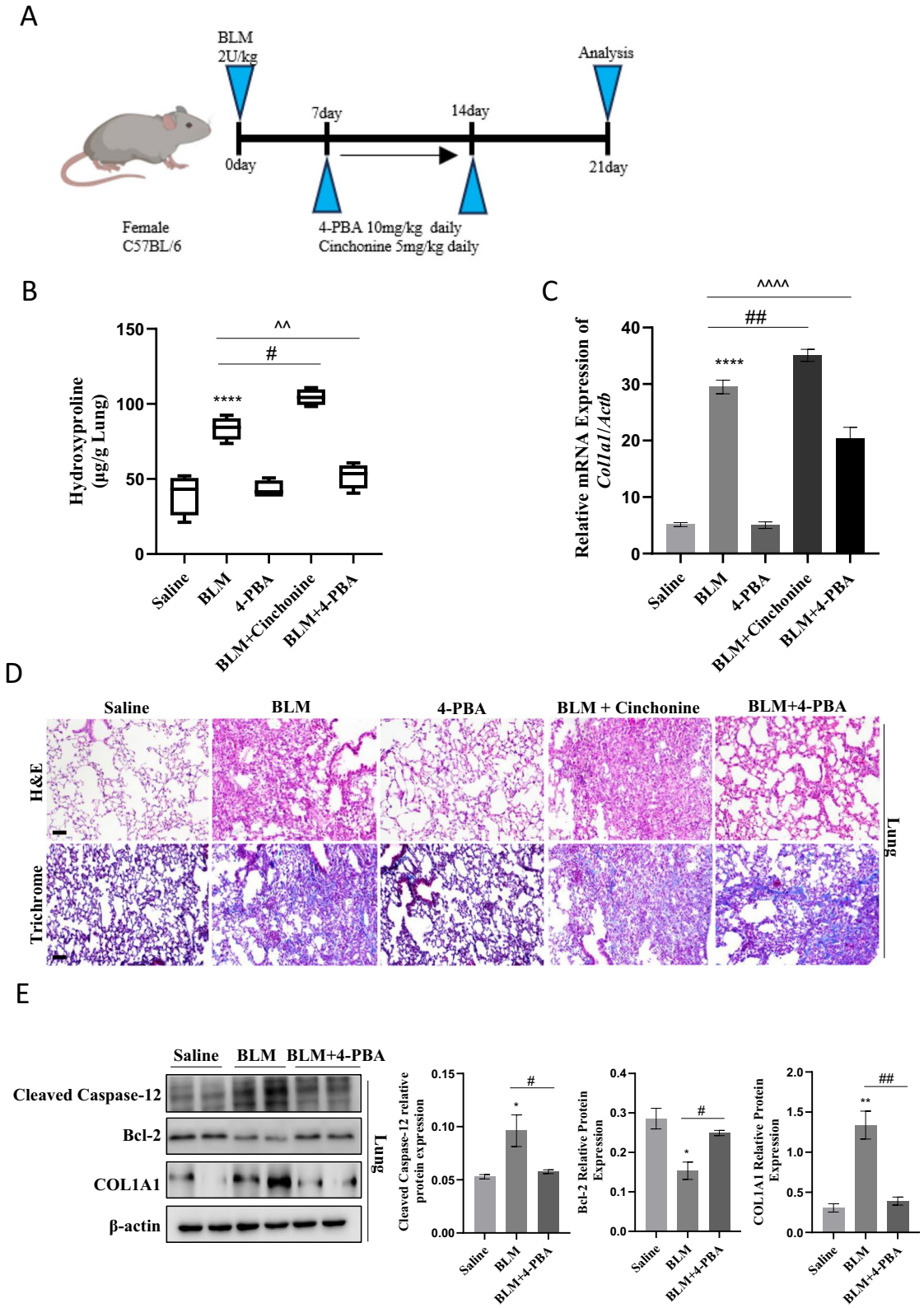

Fig. 6 (See legend on next page.)

(See figure on previous page.)

Fig. 6 ER stress inhibitor could alleviate mice pulmonary fibrosis. **A** In vivo model of PF, mice were intraperitoneally injected with 4-PBA (10mg/kg) and Cinchonine (5 mg/kg). **B** Hydroxyproline content of mice lung from Saline group, BLM group, 4-PBA group, BLM + Cinchonine and BLM + 4-PBA group. **C** The mRNA levels of *Col1a1* of mice lung were detected by qPCR. ****p < 0.0001, compared with saline group. ##p < 0.01, compared BLM group and BLM + Cinchonine group, ^^^^p < 0.0001, compared BLM group and BLM + 4-PBA group. **D** Masson's trichrome staining and H&E staining of lung sections from each group of treated mice, scale bar: 20 μm. **E** Western blot analysis the changes in protein expression of Bcl-2, Caspase-12 and COL1A1 in lung tissues treated with 4-PBA and bleomycin. *p < 0.05, **p < 0.01, compared saline group and BLM group, #p < 0.05, ##p < 0.01, compared BLM group and BLM + 4-PBA group

provided a new perspective for understanding the molecular mechanisms of PF and offers new strategies for the treatment of PF.

Supplementary Information

The online version contains supplementary material available at https://doi.org/10.1186/s12931-024-03016-5.

Supplementary Figure. (A) A549 cells were treated with TGF-β (5ng/ml) for 48h. Subsequently, the supernatant was collected and used to culture MRC-5 cells for 48 h. Western blot analysis was performed to measure the protein expression levels of N-cadherin and E-cadherin in A549 cells and Fibronectin, COL1A1, α-SMA in MRC-5 cells. (B) The mRNA levels of *Atf6* were detected by RT-qPCR (n = 3) in mice lung. ***p < 0.001, compared with saline group. (C) The mRNA expression levels of *ATF6* in A549 cells. **p < 0.01, compared with control group. (D) The morphology of the ER was detected using ER Tracker(green), Nucleus (blue), scale bar: 10μm. (E) Lactate content in BALF were measured. ****p < 0.0001, compared saline group and control group. ####p < 0.0001, compared BLM group and BLM + Cinchonine group. ^^^^p < 0.0001, compared BLM group and BLM + 4-PBA group.

Author contributions

All authors participated in manuscript revising, data analysis and giving final approval of the version to be published. ZS and JQ conceived and designed the project. WH, HM, and ZJ participated in the animal experiment. ZS and WH wrote the manuscript. ZS and JQ revised it. WH, ZJ and HM developed experimental protocols, directed the project, conceptualized and designed experiments, and interpreted results. This article was also supported to completion by GY.

Funding

This research was supported by grants from National Natural Science Foundation youth fund of China (32200714); Henan Normal University Research Launch Foundation (20220099) to Z.S; Natural Science Foundation of Henan Province (242300421535); Xinxiang Medical University Research Launch Foundation (505501) to J.Q; This research was also supported by Open Fund Project of Hebei Provincial Key Laboratory of Pulmonary Disease (2025001).

Data availability

No datasets were generated or analysed during the current study.

Declarations

Ethics approval and consent to participate

This study was carried out in accordance with the principles of the Basel Declaration and recommendations of the US NIH with Specific Pathogen Free conditions. The protocol was approved by the Model Animal Research Center of Nanjing University. All-time-available Standard rodent chow and water were also provided.

Competing interests

The authors declare no competing interests.

Received: 1 June 2024 Accepted: 19 October 2024
Published online: 09 November 2024

References

1. Sgalla G, Iovene B, Calvello M, Ori M, Varone F, Richeldi L. Idiopathic pulmonary fibrosis: pathogenesis and management. Respir Res. 2018;19:32.
2. Katzen J, Beers MF. Contributions of alveolar epithelial cell quality control to pulmonary fibrosis. J Clin Invest. 2020;130:5088–99.
3. Lederer DJ, Longo DL, Martinez FJ. Idiopathic pulmonary fibrosis. N Engl J Med. 2018;378:1811–23.
4. Ippolito L, Morandi A, Giannoni E, Chiarugi P. Lactate: a metabolic driver in the tumour landscape. Trends Biochem Sci. 2019;44:153–66.
5. Manosalva C, Quiroga J, Hidalgo AI, Alarcón P, Anseoleaga N, Hidalgo MA, Burgos RA. Role of lactate in inflammatory processes: friend or foe. Front Immunol. 2022;12:808799.
6. Kottmann RM, Kulkarni AA, Smolnycki KA, Lyda E, Dahanayake T, Salibi R, Honnons S, Jones C, Isern NG, Hu JZ, Nathan SD, Grant G, Phipps RP, Sime PJ. Lactic acid is elevated in idiopathic pulmonary fibrosis and induces myofibroblast differentiation via pH-dependent activation of transforming growth factor-β. Am J Respir Crit Care Med. 2012;186:740–51.
7. Yang L, Gilbertsen A, Xia H, Benyumov A, Smith K, Herrera J, Racila E, Bitterman PB, Henke CA. Hypoxia enhances IPF mesenchymal progenitor cell fibrogenicity via the lactate/GPR81/HIF1α pathway. JCI Insight. 2023;8:e163820.
8. Sun Z, Ji Z, He W, Duan R, Qu J, Yu G. Lactate accumulation induced by Akt2-PDK1 signaling promotes pulmonary fibrosis. FASEB J. 2024;38:e23426.
9. Newton DA, Lottes RG, Ryan RM, Spyropoulos DD, Baatz JE. Dysfunctional lactate metabolism in human alveolar type II cells from idiopathic pulmonary fibrosis lung explant tissue. Respir Res. 2021;22:278.
10. Thompson CB. Apoptosis in the pathogenesis and treatment of disease. Science. 1995;267:1456–62.
11. Nössing C, Ryan KM. 50 years on and still very much alive: "Apoptosis: a basic biological phenomenon with wide-ranging implications in tissue kinetics." Br J Cancer. 2023;128:426–31.
12. Daniel PT. Dissecting the pathways to death. Leukemia. 2000;14:2035–44.
13. Burman A, Tanjore H, Blackwell TS. Endoplasmic reticulum stress in pulmonary fibrosis. Matrix Biol. 2018;68–69:355–65.
14. du Bois RM. Evolving concepts in the early and accurate diagnosis of idiopathic pulmonary fibrosis. Clin Chest Med. 2006;27(S17–25):v–vi.
15. Uhal BD, Joshi I, Hughes WF, Ramos C, Pardo A, Selman M. Alveolar epithelial cell death adjacent to underlying myofibroblasts in advanced fibrotic human lung. Am J Physiol. 1998;275:L1192-1199.
16. Korfei M, Ruppert C, Mahavadi P, Henneke I, Markart P, Koch M, Lang G, Fink L, Bohle RM, Seeger W, Weaver TE, Guenther A. Epithelial endoplasmic reticulum stress and apoptosis in sporadic idiopathic pulmonary fibrosis. Am J Respir Crit Care Med. 2008;178:838–46.
17. Lee CG, Cho SJ, Kang MJ, Chapoval SP, Lee PJ, Noble PW, Yehualaeshet T, Lu B, Flavell RA, Milbrandt J, Homer RJ, Elias JA. Early growth response gene 1-mediated apoptosis is essential for transforming growth factor beta1-induced pulmonary fibrosis. J Exp Med. 2004;200:377–89.
18. Wallach-Dayan SB, Izbicki G, Cohen PY, Gerstl-Golan R, Fine A, Breuer R. Bleomycin initiates apoptosis of lung epithelial cells by ROS but not by Fas/FasL pathway. Am J Physiol Lung Cell Mol Physiol. 2006;290:L790-l796.
19. Chen X, Cubillos-Ruiz JR. Endoplasmic reticulum stress signals in the tumour and its microenvironment. Nat Rev Cancer. 2020;21:71–88.

20. Cubillos-Ruiz JR, Bettigole SE, Glimcher LH. Tumorigenic and immunosuppressive effects of endoplasmic reticulum stress in cancer. Cell. 2017;168:692–706.
21. Oakes SA. Endoplasmic reticulum stress signaling in cancer cells. Am J Pathol. 2020;190:934–46.
22. Burman A, Kropski JA, Calvi CL, Serezani AP, Pascoalino BD, Han W, Sherrill T, Gleaves L, Lawson WE, Young LR, Blackwell TS, Tanjore H. Localized hypoxia links ER stress to lung fibrosis through induction of C/EBP homologous protein. JCI Insight. 2018;3:e99543.
23. Shiraishi H, Okamoto H, Yoshimura A, Yoshida H. ER stress-induced apoptosis and caspase-12 activation occurs downstream of mitochondrial apoptosis involving Apaf-1. J Cell Sci. 2006;119:3958–66.
24. Kolanko E, Cargnoni A, Papait A, Silini AR, Czekaj P, Parolini O. The evolution of in vitro models of lung fibrosis: promising prospects for drug discovery. Eur Respir Rev. 2024;33:230127.
25. Galluzzi L, Kepp O, Kroemer G. Reverse Warburg: straight to cancer. Cell Cycle. 2012;11:1059–1059.
26. Mao N, Fan Y, Liu W, Yang H, Yang Y, Li Y, Jin F, Li T, Yang X, Gao X, Cai W, Liu H, Xu H, Li S, Yang F. Oxamate attenuates glycolysis and ER stress in silicotic mice. Int J Mol Sci. 2022;23:3013.
27. Kim C, Kim B. Anti-cancer natural products and their bioactive compounds inducing ER stress-mediated apoptosis: a review. Nutrients. 2018;10:1021.
28. Varone E, Decio A, Chernorudskiy A, Minoli L, Brunelli L, Ioli F, Piotti A, Pastorelli R, Fratelli M, Gobbi M, Giavazzi R, Zito E. The ER stress response mediator ERO1 triggers cancer metastasis by favoring the angiogenic switch in hypoxic conditions. Oncogene. 2021;40:1721–36.
29. Schwarz DS, Blower MD. The endoplasmic reticulum: structure, function and response to cellular signaling. Cell Mol Life Sci. 2016;73:79–94.
30. Roberson EC, Tully JE, Guala AS, Reiss JN, Godburn KE, Pociask DA, Alcorn JF, Riches DW, Dienz O, Janssen-Heininger YM, Anathy V. Influenza induces endoplasmic reticulum stress, caspase-12-dependent apoptosis, and c-Jun N-terminal kinase-mediated transforming growth factor-beta release in lung epithelial cells. Am J Respir Cell Mol Biol. 2012;46:573–81.
31. Dai J, Liu J, Shen Y, Zhang B, Li C, Liu Z. Regulation of endoplasmic reticulum stress on autophagy and apoptosis of nucleus pulposus cells in intervertebral disc degeneration and its related mechanisms. PeerJ. 2024;12: e17212.
32. Wang S, Xu F, Liu H, Shen Y, Zhang J, Hu L, Zhu L. Suppressing endoplasmic reticulum stress alleviates LPS-induced acute lung injury via inhibiting inflammation and ferroptosis. Inflammation. 2024;47:1067–82.
33. Hu H, Fan X, Guo Q, Wei X, Yang D, Zhang B, Liu J, Wu Q, Oh Y, Feng Y, Chen K, Hou L, Gu N. Silicon dioxide nanoparticles induce insulin resistance through endoplasmic reticulum stress and generation of reactive oxygen species. Part Fibre Toxicol. 2019;16:41.
34. Yuan H, He Y, Zhang Y, Min H, Chen J, Li C. Crystalline silica-induced endoplasmic reticulum stress promotes the pathogenesis of silicosis by augmenting proinflammatory interstitial pulmonary macrophages. Sci Total Environ. 2024;946: 174299.
35. Ma J, Wang J, Ma C, Cai Q, Wu S, Hu W, Yang J, Xue J, Chen J, Liu X. Wnt5a/Ca(2+) signaling regulates silica-induced ferroptosis in mouse macrophages by altering ER stress-mediated redox balance. Toxicology. 2023;490: 153514.
36. Dai E, Wang W, Li Y, Ye D, Li Y. Lactate and lactylation: behind the development of tumors. Cancer Lett. 2024;591: 216896.

Publisher's Note